

Experiment Simulation Configurations Approximating DUNE TDR

- B. Abi,¹⁴⁰ R. Acciarri,⁶¹ M. A. Acero,⁸ G. Adamov,⁶⁵ D. Adams,¹⁷ M. Adinolfi,¹⁶ Z. Ahmad,¹⁷⁹ J. Ahmed,¹⁸² T. Alion,¹⁶⁸ S. Alonso Monsalve,²¹ C. Alt,⁵³ J. Anderson,⁴ C. Andreopoulos,¹⁸⁹ M. P. Andrews,⁶¹ F. Andrianala,² S. Andringa,¹¹³ A. Ankowski,¹⁵⁸ M. Antonova,⁷⁷ S. Antusch,¹⁰ A. Aranda-Fernandez,³⁹ A. Ariga,¹¹ L. O. Arnold,⁴² M. A. Arroyave,⁵² J. Asaadi,¹⁷² A. Aurisano,³⁷ V. Aushev,¹¹² D. Autiero,⁸⁹ F. Azfar,¹⁴⁰ H. Back,¹⁴¹ J. J. Back,¹⁸² C. Backhouse,¹⁷⁷ P. Baesso,¹⁶ L. Bagby,⁶¹ R. Bajou,¹⁴³ S. Balasubramanian,¹⁸⁶ P. Baldi,²⁶ B. Bambah,⁷⁵ F. Barao,¹⁹⁰ G. Barenboim,⁷⁷ G. J. Barker,¹⁸² W. Barkhouse,¹³⁴ C. Barnes,¹²⁴ G. Barr,¹⁴⁰ J. Barranco Monarca,⁷⁰ N. Barros,¹⁹¹ J. L. Barrow,¹⁹² A. Bashyal,¹³⁹ V. Basque,¹²² F. Bay,¹³³ J. L. Bazo Alba,¹⁵⁰ J. F. Beacom,¹³⁸ E. Bechettoile,⁸⁹ B. Behera,⁴¹ L. Bellantoni,⁶¹ G. Bellettini,¹⁴⁸ V. Bellini,¹⁹³ O. Beltramello,²¹ D. Belver,²² N. Benekos,²¹ F. Bento Neves,¹¹³ J. Berger,¹⁴⁹ S. Berkman,⁶¹ P. Bernardini,¹⁹⁴ R. M. Berner,¹¹ H. Berns,²⁵ S. Bertolucci,¹⁹⁵ M. Betancourt,⁶¹ Y. Bezawada,²⁵ M. Bhattacharjee,⁹⁵ B. Bhuyan,⁹⁵ S. Biagi,⁸⁷ J. Bian,²⁶ M. Biassoni,⁸² K. Biery,⁶¹ B. Bilki,¹⁹⁶ M. Bishai,¹⁷ A. Bitadze,¹²² A. Blake,¹¹⁵ B. Blanco Siffert,⁶⁰ F. D. M. Blaszczyk,⁶¹ G. C. Blazey,¹³⁵ E. Blucher,³⁵ J. Boissevain,¹¹⁸ S. Bolognesi,²⁰ T. Bolton,¹⁰⁹ M. Bonesini,¹⁹⁷ M. Bongrand,¹¹⁴ F. Bonini,¹⁷ A. Booth,¹⁶⁸ C. Booth,¹⁶² S. Bordoni,²¹ A. Borkum,¹⁶⁸ T. Boschi,⁵¹ N. Bostan,⁹⁹ P. Bour,⁴⁴ S. B. Boyd,¹⁸² D. Boyden,¹³⁵ J. Bracinik,¹³ D. Braga,⁶¹ D. Brailsford,¹¹⁵ A. Brandt,¹⁷² J. Bremer,²¹ C. Brew,¹⁵⁷ E. Brianne,¹²² S. J. Brice,⁶¹ C. Brizzolari,¹⁹⁷ C. Bromberg,¹²⁵ G. Brooijmans,⁴² J. Brooke,¹⁶ A. Gross,⁶¹ G. Brunetti,⁸⁵ N. Buchanan,⁴¹ H. Budd,¹⁵⁴ D. Caiulo,⁸⁹ P. Calafiura,¹¹⁶ J. Calcutt,¹²⁵ M. Calin,¹⁸ S. Calvez,⁴¹ E. Calvo,²² L. Camilleri,⁴² A. Caminata,⁸⁰ M. Campanelli,¹⁷⁷ D. Caratelli,⁶¹ G. Carini,¹⁷ B. Carlus,⁸⁹ P. Carniti,⁸² I. Caro Terrazas,⁴¹ H. Carranza,¹⁷² A. Castillo,¹⁶¹ C. Castromonte,⁹⁸ C. Cattadori,⁸² F. Cavalier,¹¹⁴ F. Cavanna,⁶¹ S. Centro,¹⁴² G. Cerati,⁶¹ A. Cervelli,⁷⁸ A. Cervera Villanueva,⁷⁷ M. Chalifour,²¹ C. Chang,²⁸ E. Chardonnet,¹⁴³ A. Chatterjee,¹⁴⁹ S. Chattopadhyay,¹⁷⁹ J. Chaves,¹⁴⁵ H. Chen,¹⁷ M. Chen,²⁶ Y. Chen,¹¹ D. Cherdack,⁷⁴ C. Chi,⁴² S. Childress,⁶¹ A. Chiriacescu,¹⁸ K. Cho,¹⁰⁷ S. Choubey,⁷¹ A. Christensen,⁴¹ D. Christian,⁶¹ G. Christodoulou,²¹ E. Church,¹⁴¹ P. Clarke,⁵⁴ T. E. Coan,¹⁶⁶ A. G. Cocco,⁸⁴ J. A. B. Coelho,¹¹⁴ E. Conley,⁵⁰ J. M. Conrad,¹²³ M. Convery,¹⁵⁸ L. Corwin,¹⁶³ P. Cotte,²⁰ L. Cremaldi,¹³⁰ L. Cremonesi,¹⁷⁷ J. I. Crespo-Anadón,²² E. Cristaldo,⁶ R. Cross,¹¹⁵ C. Cuesta,²² Y. Cui,²⁸ D. Cussans,¹⁶ M. Dabrowski,¹⁷ H. da Motta,¹⁹ L. Da Silva Peres,⁶⁰ C. David,¹⁹⁸ Q. David,⁸⁹ G. S. Davies,¹³⁰ S. Davini,⁸⁰ J. Dawson,¹⁴³ K. De,¹⁷² R. M. De Almeida,⁶³ P. Debbins,⁹⁹ I. De Bonis,⁴⁷ M. P. Decowski,¹⁹⁹ A. de Gouvêa,¹³⁶ P. C. De Holanda,³² I. L. De Icaza Astiz,¹⁶⁸ A. Deisting,¹⁵⁵ P. De Jong,¹⁹⁹ A. Delbart,²⁰ D. Delepine,⁷⁰ M. Delgado,³ A. Dell'Acqua,²¹ P. De Lurgio,⁴ J. R. T. de Mello Neto,⁶⁰ D. M. DeMuth,¹⁷⁸ S. Dennis,³¹ C. Densham,¹⁵⁷ G. Deptuch,⁶¹ A. De Roeck,²¹ V. De Romeri,⁷⁷ J. J. De Vries,³¹ R. Dharmapalan,⁷³ M. Dias,¹⁷⁶ F. Diaz,¹⁵⁰ J. S. Diaz,⁹⁷ S. Di Domizio,²⁰⁰ L. Di Giulio,²¹ P. Ding,⁶¹ L. Di Noto,²⁰⁰ C. Distefano,⁸⁷ R. Diurba,¹²⁹ M. Diwan,¹⁷ Z. Djurcic,⁴ N. Dokania,¹⁶⁷ M. J. Dolinski,⁴⁹ L. Domine,¹⁵⁸ D. Douglas,¹²⁵ F. Drielsma,¹⁵⁸ D. Duchesneau,⁴⁷ K. Duffy,⁶¹ P. Dunne,⁹⁴ T. Durkin,¹⁵⁷ H. Duyang,¹⁶⁵ O. Dvornikov,⁷³ D. A. Dwyer,¹¹⁶ A. S. Dyshkant,¹³⁵ M. Eads,¹³⁵ D. Edmunds,¹²⁵ J. Eisch,¹⁰⁰ S. Emery,²⁰ A. Ereditato,¹¹ C. O. Escobar,⁶¹ L. Escudero Sanchez,³¹ J. J. Evans,¹²² E. Ewart,⁹⁷ A. C. Ezeribe,¹⁶² K. Fahey,⁶¹ A. Falcone,¹⁹⁷ C. Farnese,¹⁴² Y. Farzan,⁹⁰ J. Felix,⁷⁰ E. Fernandez-Martinez,¹²¹ P. Fernandez Menendez,⁷⁷ F. Ferraro,²⁰⁰ L. Fields,⁶¹ A. Filkins,¹⁸⁴ F. Filthaut,²⁰¹ R. S. Fitzpatrick,¹²⁴ W. Flanagan,⁴⁶ B. Fleming,¹⁸⁶ R. Flight,¹⁵⁴ J. Fowler,⁵⁰ W. Fox,⁹⁷ J. Franc,⁴⁴ K. Francis,¹³⁵ D. Franco,¹⁸⁶ J. Freeman,⁶¹ J. Freestone,¹²² J. Fried,¹⁷ A. Friedland,¹⁵⁸ S. Fuess,⁶¹ I. Furic,⁶² A. P. Furmanski,¹²⁹ A. Gago,¹⁵⁰ H. Gallagher,¹⁷⁵ A. Gallego-Ros,²² N. Gallice,²⁰² V. Galymov,⁸⁹ E. Gamberini,²¹ T. Gamble,¹⁶² R. Gandhi,⁷¹ R. Gandrajula,¹²⁵ S. Gao,¹⁷ D. Garcia-Gamez,⁶⁸ M. Á. García-Peris,⁷⁷ S. Gardiner,⁶¹ D. Gastler,¹⁵ G. Ge,⁴² B. Gelli,³² A. Gendotti,⁵³ S. Gent,¹⁶⁴ Z. Ghorbani-Moghaddam,⁸⁰ D. Gibin,¹⁴² I. Gil-Botella,²² C. Girerd,⁸⁹ A. K. Giri,⁹⁶ D. Gnani,¹¹⁶ O. Gogota,¹¹² M. Gold,¹³¹ S. Gollapinni,¹¹⁸ K. Gollwitzer,⁶¹ R. A. Gomes,⁵⁷ L. V. Gomez Bermeo,¹⁶¹ L. S. Gomez Fajardo,¹⁶¹ F. Gonnella,¹³ J. A. Gonzalez-Cuevas,⁶ M. C. Goodman,⁴ O. Goodwin,¹²² S. Goswami,¹⁴⁷ C. Gotti,⁸² E. Goudzovski,¹³ C. Grace,¹¹⁶ M. Graham,¹⁵⁸ E. Gramellini,¹⁸⁶ R. Gran,¹²⁸ E. Granados,⁷⁰ A. Grant,⁴⁸ C. Grant,¹⁵ D. Gratieri,⁶³ P. Green,¹²² S. Green,³¹ L. Greenler,¹⁸⁵ M. Greenwood,¹³⁹ J. Greer,¹⁶ W. C. Griffith,¹⁶⁸ M. Groh,⁹⁷ J. Grudzinski,⁴ K. Grzelak,¹⁸¹ W. Gu,¹⁷ V. Guarino,⁴ R. Guenette,⁷² A. Guglielmi,⁸⁵ B. Guo,¹⁶⁵ K. K. Guthikonda,¹⁰⁸ R. Gutierrez,³ P. Guzowski,¹²² M. M. Guzzo,³² S. Gwon,³⁶ A. Habig,¹²⁸ A. Hackenburg,¹⁸⁶ H. Hadavand,¹⁷² R. Haenni,¹¹ A. Hahn,⁶¹ J. Haigh,¹⁸² J. Haiston,¹⁶³ T. Hamernik,⁶¹ P. Hamilton,⁹⁴ J. Han,¹⁴⁹ K. Harder,¹⁵⁷ D. A. Harris,¹⁹⁸ J. Hartnell,¹⁶⁸ T. Hasegawa,¹⁰⁶ R. Hatcher,⁶¹ E. Hazen,¹⁵ A. Heavey,⁶¹ K. M. Heeger,¹⁸⁶ J. Heise,¹⁵⁹ K. Hennessy,¹¹⁷ S. Henry,¹⁵⁴ M. A. Hernandez Morquecho,⁷⁰ K. Herner,⁶¹ L. Hertel,²⁶ A. S. Hesam,²¹ V. Hewes,³⁷ A. Higuera,⁷⁴ T. Hill,⁹² S. J. Hillier,¹³ A. Himmel,⁶¹ J. Hoff,⁶¹ C. Hohl,¹⁰ A. Holin,¹⁷⁷ E. Hoppe,¹⁴¹ G. A. Horton-Smith,¹⁰⁹ M. Hostert,⁵¹ A. Hourlier,¹²³ B. Howard,⁶¹ R. Howell,¹⁵⁴ J. Huang,¹⁷³ J. Huang,²⁵ J. Hugon,¹¹⁹ G. Iles,⁹⁴ N. Ilie,¹⁷⁴ A. M. Iliescu,⁷⁸ R. Illingworth,⁶¹ A. Ioannisian,¹⁸⁷ R. Itay,¹⁵⁸

- A. Izmaylov,⁷⁷ E. James,⁶¹ B. Jargowsky,²⁶ F. Jediny,⁴⁴ C. Jesùs-Valls,⁷⁶ X. Ji,¹⁷ L. Jiang,¹⁸⁰ S. Jiménez,²²
 A. Jipa,¹⁸ A. Joglekar,²⁸ C. Johnson,⁴¹ R. Johnson,³⁷ B. Jones,¹⁷² S. Jones,¹⁷⁷ C. K. Jung,¹⁶⁷ T. Junk,⁶¹ Y. Jwa,⁴²
 M. Kabirnezhad,¹⁴⁰ A. Kaboth,¹⁵⁷ I. Kadenko,¹¹² F. Kamiya,⁵⁹ G. Karagiorgi,⁴² A. Karcher,¹¹⁶ M. Karolak,²⁰
 Y. Karyotakis,⁴⁷ S. Kasai,¹¹¹ S. P. Kasetti,¹¹⁹ L. Kashur,⁴¹ N. Kazaryan,¹⁸⁷ E. Kearns,¹⁵ P. Keener,¹⁴⁵ K.J. Kelly,⁶¹
 E. Kemp,³² W. Ketchum,⁶¹ S. H. Kettell,¹⁷ M. Khabibullin,⁸⁸ A. Khotjantsev,⁸⁸ A. Khvedelidze,⁶⁵ D. Kim,²¹
 B. King,⁶¹ B. Kirby,¹⁷ M. Kirby,⁶¹ J. Klein,¹⁴⁵ K. Koehler,¹⁸⁵ L. W. Koerner,⁷⁴ S. Kohn,²⁰³ P. P. Koller,¹¹
 M. Kordosky,¹⁸⁴ T. Kosc,⁸⁹ U. Kose,²¹ V. A. Kostelecký,⁹⁷ K. Kotekar,¹⁶ F. Krennrich,¹⁰⁰ I. Kreslo,¹¹
 Y. Kudenko,⁸⁸ V. A. Kudryavtsev,¹⁶² S. Kulagin,⁸⁸ J. Kumar,⁷³ R. Kumar,¹⁵² C. Kuruppu,¹⁶⁵ V. Kus,⁴⁴
 T. Kutter,¹¹⁹ A. Lambert,¹¹⁶ K. Lande,¹⁴⁵ C. E. Lane,⁴⁹ K. Lang,¹⁷³ T. Langford,¹⁸⁶ P. Lasorak,¹⁶⁸ D. Last,¹⁴⁵
 C. Lastoria,²² A. Laundrie,¹⁸⁵ A. Lawrence,¹¹⁶ I. Lazanu,¹⁸ R. LaZur,⁴¹ T. Le,¹⁷⁵ J. Learned,⁷³ P. LeBrun,⁸⁹
 G. Lehmann Miotto,²¹ R. Lehnert,⁹⁷ M. A. Leogui de Oliveira,⁵⁹ M. Leitner,¹¹⁶ M. Leyton,⁷⁶ L. Li,²⁶ S. Li,¹⁷
 S. W. Li,¹⁵⁸ T. Li,⁵⁴ Y. Li,¹⁷ H. Liao,¹⁰⁹ C. S. Lin,¹¹⁶ S. Lin,¹¹⁹ A. Lister,¹⁸⁵ B. R. Littlejohn,⁹³ J. Liu,²⁶
 S. Lockwitz,⁶¹ T. Loew,¹¹⁶ M. Lokajicek,⁴³ I. Lomidze,⁶⁵ K. Long,⁹⁴ K. Loo,¹⁰⁵ D. Lorca,¹¹ T. Lord,¹⁸²
 J. M. LoSecco,¹³⁷ W. C. Louis,¹¹⁸ K.B. Luk,²⁰³ X. Luo,²⁹ N. Lurkin,¹³ T. Lux,⁷⁶ V. P. Luzio,⁵⁹ D. MacFarland,¹⁵⁸
 A. A. Machado,³² P. Machado,⁶¹ C. T. Macias,⁹⁷ J. R. Macier,⁶¹ A. Maddalena,⁶⁷ P. Madigan,²⁰³ S. Magill,⁴
 K. Mahn,¹²⁵ A. Maio,¹⁹¹ J. A. Maloney,⁴⁵ G. Mandrioli,⁷⁸ J. Maneira,¹⁹¹ L. Manenti,¹⁷⁷ S. Manly,¹⁵⁴ A. Mann,¹⁷⁵
 K. Manolopoulos,¹⁵⁷ M. Manrique Plata,⁹⁷ A. Marchionni,⁶¹ W. Marciano,¹⁷ D. Marfatia,⁷³ C. Mariani,¹⁸⁰
 J. Maricic,⁷³ F. Marinho,⁵⁸ A. D. Marino,⁴⁰ M. Marshak,¹²⁹ C. Marshall,¹¹⁶ J. Marshall,¹⁸² J. Marteau,⁸⁹
 J. Martin-Albo,⁷⁷ N. Martinez,¹⁰⁹ D.A. Martinez Caicedo,¹⁶³ S. Martynenko,¹⁶⁷ K. Mason,¹⁷⁵ A. Mastbaum,¹⁵⁶
 M. Masud,⁷⁷ S. Matsuno,⁷³ J. Matthews,¹¹⁹ C. Mauger,¹⁴⁵ N. Mauri,¹⁹⁵ K. Mavrokordis,¹¹⁷ R. Mazza,⁸²
 A. Mazzacane,⁶¹ E. Mazzucato,²⁰ E. McCluskey,⁶¹ N. McConkey,¹²² K. S. McFarland,¹⁵⁴ C. McGrew,¹⁶⁷
 A. McNab,¹²² A. Mefodiev,⁸⁸ P. Mehta,¹⁰³ P. Melas,⁷ M. Mellinato,¹⁹⁷ O. Mena,⁷⁷ S. Menary,¹⁸⁸ H. Mendez,¹⁵¹
 A. Menegolli,²⁰⁴ G. Meng,⁸⁵ M. D. Messier,⁹⁷ W. Metcalf,¹¹⁹ M. Mewes,⁹⁷ H. Meyer,¹⁸³ T. Miao,⁶¹ G. Michna,¹⁶⁴
 T. Miedema,²⁰¹ J. Migenda,¹⁶² R. Milincic,⁷³ W. Miller,¹²⁹ J. Mills,¹⁷⁵ C. Milne,⁹² O. Mineev,⁸⁸ O. G. Miranda,³⁸
 S. Miryala,¹⁷ C. S. Mishra,⁶¹ S. R. Mishra,¹⁶⁵ A. Mislivec,¹²⁹ D. Mladenov,²¹ I. Mocioiu,¹⁴⁶ K. Moffat,⁵¹
 N. Moggi,¹⁹⁵ R. Mohanta,⁷⁵ T. A. Mohayai,⁶¹ N. Mokhov,⁶¹ J. Molina,⁶ L. Molina Bueno,⁵³ A. Montanari,⁷⁸
 C. Montanari,²⁰⁴ D. Montanari,⁶¹ L. M. Montano Zetina,³⁸ J. Moon,¹²³ M. Mooney,⁴¹ A. Moor,³¹ D. Moreno,³
 B. Morgan,¹⁸² C. Morris,⁷⁴ C. Mossey,⁶¹ E. Motuk,¹⁷⁷ C. A. Moura,⁵⁹ J. Mousseau,¹²⁴ W. Mu,⁶¹ L. Mualem,³⁰
 J. Mueller,⁴¹ M. Muether,¹⁸³ S. Mufson,⁹⁷ F. Muheim,⁵⁴ A. Muir,⁴⁸ M. Mulhearn,²⁵ H. Muramatsu,¹²⁹
 S. Murphy,⁵³ J. Musser,⁹⁷ J. Nachtman,⁹⁹ S. Nagu,¹²⁰ M. Nalbandyan,¹⁸⁷ R. Nandakumar,¹⁵⁷ D. Naples,¹⁴⁹
 S. Narita,¹⁰¹ D. Navas-Nicolás,²² N. Nayak,²⁶ M. Nebot-Guinot,⁵⁴ L. Necib,³⁰ K. Negishi,¹⁰¹ J. K. Nelson,¹⁸⁴
 J. Nesbit,¹⁸⁵ M. Nessi,²¹ D. Newbold,¹⁵⁷ M. Newcomer,¹⁴⁵ D. Newhart,⁶¹ R. Nichol,¹⁷⁷ E. Niner,⁶¹ K. Nishimura,⁷³
 A. Norman,⁶¹ A. Norrick,⁶¹ R. Northrop,³⁵ P. Novella,⁷⁷ J. A. Nowak,¹¹⁵ M. Oberling,⁴ A. Olivares Del Campo,⁵¹
 A. Olivier,¹⁵⁴ Y. Onel,⁹⁹ Y. Onishchuk,¹¹² J. Ott,²⁶ L. Pagani,²⁵ S. Pakvasa,⁷³ O. Palamara,⁶¹ S. Palestini,²¹
 J. M. Paley,⁶¹ M. Pallavicini,²⁰⁰ C. Palomares,²² E. Pantic,²⁵ V. Paolone,¹⁴⁹ V. Papadimitriou,⁶¹ R. Papaleo,⁸⁷
 A. Papanestis,¹⁵⁷ S. Paramesvaran,¹⁶ S. Parke,⁶¹ Z. Parsa,¹⁷ M. Parvu,¹⁸ S. Pascoli,⁵¹ L. Pasqualini,¹⁹⁵
 J. Pasternak,⁹⁴ J. Pater,¹²² C. Patrick,¹⁷⁷ L. Patrizii,⁷⁸ R. B. Patterson,³⁰ S. J. Patton,¹¹⁶ T. Patzak,¹⁴³
 A. Paudel,¹⁰⁹ B. Paulos,¹⁸⁵ L. Paulucci,⁵⁹ Z. Pavlovic,⁶¹ G. Pawloski,¹²⁹ D. Payne,¹¹⁷ V. Pec,¹⁶² S. J. M. Peeters,¹⁶⁸
 Y. Penichot,²⁰ E. Pennacchio,⁸⁹ A. Penzo,⁹⁹ O. L. G. Peres,³² J. Perry,⁵⁴ D. Pershey,⁵⁰ G. Pessina,⁸² G. Petrillo,¹⁵⁸
 C. Petta,¹⁹³ R. Petti,¹⁶⁵ F. Piastra,¹¹ L. Pickering,¹²⁵ F. Pietropaolo,²⁰⁵ J. Pillow,¹⁸² J. Pinzino,¹⁷⁴ R. Plunkett,⁶¹
 R. Poling,¹²⁹ X. Pons,²¹ N. Poonthottathil,¹⁰⁰ S. Pordes,⁶¹ M. Potekhin,¹⁷ R. Potenza,¹⁹³ B. V. K. S. Potukuchi,¹⁰²
 J. Pozimski,⁹⁴ M. Pozzato,¹⁹⁵ S. Prakash,³² T. Prakash,¹¹⁶ S. Prince,⁷² G. Prior,¹¹³ D. Pugnere,⁸⁹ K. Qi,¹⁶⁷
 X. Qian,¹⁷ J. L. Raaf,⁶¹ R. Raboanary,² V. Radeka,¹⁷ J. Rademacker,¹⁶ B. Radics,⁵³ A. Rafique,⁴ E. Raguzin,¹⁷
 M. Rai,¹⁸² M. Rajaoalisoa,³⁷ I. Rakhno,⁶¹ H. T. Rakotondramanana,² L. Rakotondravohitra,² Y. A. Ramachers,¹⁸²
 R. Rameika,⁶¹ M. A. Ramirez Delgado,⁷⁰ B. Ramson,⁶¹ A. Rappoldi,²⁰⁴ G. Raselli,²⁰⁴ P. Ratoff,¹¹⁵ S. Ravat,²¹
 H. Razafinime,² J.S. Real,⁶⁹ B. Rebel,²⁰⁶ D. Redondo,²² M. Reggiani-Guzzo,³² T. Rehak,⁴⁹ J. Reichenbacher,¹⁶³
 S. D. Reitzner,⁶¹ A. Renshaw,⁷⁴ S. Rescia,¹⁷ F. Resnati,²¹ A. Reynolds,¹⁴⁰ G. Riccobene,⁸⁷ L. C. J. Rice,¹⁴⁹
 K. Rielage,¹¹⁸ Y. Rigaut,⁵³ D. Rivera,¹⁴⁵ L. Rochester,¹⁵⁸ M. Roda,¹¹⁷ P. Rodrigues,¹⁴⁰ M. J. Rodriguez Alonso,²¹
 J. Rodriguez Rondon,¹⁶³ A. J. Roeth,⁵⁰ H. Rogers,⁴¹ S. Rosauro-Alcaraz,¹²¹ M. Rossella,²⁰⁴ J. Rout,¹⁰³ S. Roy,⁷¹
 A. Rubbia,⁵³ C. Rubbia,⁶⁶ B. Russell,¹¹⁶ J. Russell,¹⁵⁸ D. Ruterborries,¹⁵⁴ R. Saakyan,¹⁷⁷ S. Sacerdoti,¹⁴³
 T. Safford,¹²⁵ N. Sahu,⁹⁶ P. Sala,²⁰⁷ N. Samios,¹⁷ M. C. Sanchez,¹⁰⁰ D. A. Sanders,¹³⁰ D. Sankey,¹⁵⁷ S. Santana,¹⁵¹
 M. Santos-Maldonado,¹⁵¹ N. Saoulidou,⁷ P. Sapienza,⁸⁷ C. Sarasty,³⁷ I. Sarcevic,⁵ G. Savage,⁶¹ V. Savinov,¹⁴⁹
 A. Scaramelli,⁸⁶ A. Scarff,¹⁶² A. Scarpelli,¹⁷ T. Schaffer,¹²⁸ H. Schellman,²⁰⁸ P. Schlabaach,⁶¹ D. Schmitz,³⁵

K. Scholberg,⁵⁰ A. Schukraft,⁶¹ E. Segreto,³² J. Sensenig,¹⁴⁵ I. Seong,²⁶ A. Sergi,¹³ F. Sergiampietri,¹⁶⁷
D. Sgalaberna,⁵³ M. H. Shaevitz,⁴² S. Shafaq,¹⁰³ M. Shamma,²⁸ H. R. Sharma,¹⁰² R. Sharma,¹⁷ T. Shaw,⁶¹
C. Shepherd-Themistocleous,¹⁵⁷ S. Shin,¹⁰⁴ D. Shultz,¹²⁵ R. Shrock,¹⁶⁷ L. Simard,¹¹⁴ N. Simos,¹⁷ J. Sinclair,¹¹
G. Sinev,⁵⁰ J. Singh,¹²⁰ J. Singh,¹²⁰ V. Singh,²⁰⁹ R. Sipos,²¹ F. W. Sippach,⁴² G. Sirri,⁷⁸ A. Sitraka,¹⁶³ K. Siyeon,³⁶
D. Smargianaki,¹⁶⁷ A. Smith,⁵⁰ A. Smith,³¹ E. Smith,⁹⁷ P. Smith,⁹⁷ J. Smolik,⁴⁴ M. Smy,²⁶ P. Snopok,⁹³ M. Soares
Nunes,³² H. Sobel,²⁶ M. Soderberg,¹⁶⁹ C. J. Solano Salinas,⁹⁸ S. Söldner-Rembold,¹²² N. Solomey,¹⁸³ V. Solovov,¹¹³
W. E. Sondheim,¹¹⁸ M. Sorel,⁷⁷ J. Soto-Oton,²² A. Sousa,³⁷ K. Soustruznik,³⁴ F. Spagliardi,¹⁴⁰ M. Spanu,¹⁷
J. Spitz,¹²⁴ N. J. C. Spooner,¹⁶² K. Spurgeon,¹⁶⁹ R. Staley,¹³ M. Stancari,⁶¹ L. Stanco,⁸⁵ H. M. Steiner,¹¹⁶
J. Stewart,¹⁷ B. Stillwell,³⁵ J. Stock,¹⁶³ F. Stocker,²¹ T. Stokes,¹¹⁹ M. Strait,¹²⁹ T. Strauss,⁶¹ S. Striganov,⁶¹
A. Stuart,³⁹ D. Summers,¹³⁰ A. Surdo,⁸¹ V. Susic,¹⁰ L. Suter,⁶¹ C. M. Sutera,¹⁹³ R. Svoboda,²⁵ B. Szczerbinska,¹⁷¹
A. M. Szelc,¹²² R. Talaga,⁴ H. A. Tanaka,¹⁵⁸ B. Tapia Oregui,¹⁷³ A. Tapper,⁹⁴ S. Tariq,⁶¹ E. Tatar,⁹² R. Tayloe,⁹⁷
A. M. Teklu,¹⁶⁷ M. Tenti,⁷⁸ K. Terao,¹⁵⁸ C. A. Ternes,⁷⁷ F. Terranova,¹⁹⁷ G. Testera,⁸⁰ A. Thea,¹⁵⁷
J. L. Thompson,¹⁶² C. Thorn,¹⁷ S. C. Timm,⁶¹ A. Tonazzo,¹⁴³ M. Torti,¹⁹⁷ M. Tortola,⁷⁷ F. Tortorici,¹⁹³
D. Totani,⁶¹ M. Toups,⁶¹ C. Touramanis,¹¹⁷ J. Trevor,³⁰ W. H. Trzaska,¹⁰⁵ Y. T. Tsai,¹⁵⁸ Z. Tsamalaidze,⁶⁵
K. V. Tsang,¹⁵⁸ N. Tsverava,⁶⁵ S. Tufanli,²¹ C. Tull,¹¹⁶ E. Tyley,¹⁶² M. Tzanov,¹¹⁹ M. A. Uchida,³¹ J. Urheim,⁹⁷
T. Usher,¹⁵⁸ M. R. Vagins,¹¹⁰ P. Vahle,¹⁸⁴ G. A. Valdivieso,⁵⁶ E. Valencia,¹⁸⁴ Z. Vallari,³⁰ J. W. F. Valle,⁷⁷
S. Vallecorsa,²¹ R. Van Berg,¹⁴⁵ R. G. Van de Water,¹¹⁸ D. Vanegas Forero,³² F. Varanini,⁸⁵ D. Vargas,⁷⁶
G. Varner,⁷³ J. Vasel,⁹⁷ G. Vasseur,²⁰ K. Vaziri,⁶¹ S. Ventura,⁸⁵ A. Verdugo,²² S. Vergani,³¹ M. A. Vermeulen,¹³³
M. Verzocchi,⁶¹ H. Vieira de Souza,³² C. Vignoli,⁶⁷ C. Vilela,¹⁶⁷ B. Viren,¹⁷ T. Vrba,⁴⁴ T. Wachala,¹³²
A. V. Waldron,⁹⁴ M. Wallbank,³⁷ H. Wang,²⁷ J. Wang,²⁵ Y. Wang,²⁷ Y. Wang,¹⁶⁷ K. Warburton,¹⁰⁰ D. Warner,⁴¹
M. Wascko,⁹⁴ D. Waters,¹⁷⁷ A. Watson,¹³ P. Weatherly,⁴⁹ A. Weber,²¹⁰ M. Weber,¹¹ H. Wei,¹⁷ A. Weinstein,¹⁰⁰
D. Wenman,¹⁸⁵ M. Wetstein,¹⁰⁰ M. R. While,¹⁶³ A. White,¹⁷² L. H. Whitehead,³¹ D. Whittington,¹⁶⁹
M. J. Wilking,¹⁶⁷ C. Wilkinson,¹¹ Z. Williams,¹⁷² F. Wilson,¹⁵⁷ R. J. Wilson,⁴¹ J. Wolcott,¹⁷⁵ T. Wongjirad,¹⁷⁵
K. Wood,¹⁶⁷ L. Wood,¹⁴¹ E. Worcester,¹⁷ M. Worcester,¹⁷ C. Wret,¹⁵⁴ W. Wu,⁶¹ W. Wu,²⁶ Y. Xiao,²⁶ G. Yang,¹⁶⁷
T. Yang,⁶¹ N. Yershov,⁸⁸ K. Yonehara,⁶¹ T. Young,¹³⁴ B. Yu,¹⁷ J. Yu,¹⁷² R. Zaki,¹⁸⁸ J. Zalesak,⁴³ L. Zambelli,⁴⁷
B. Zamorano,⁶⁸ A. Zani,⁸³ L. Zazueta,¹⁸⁴ G. P. Zeller,⁶¹ J. Zennamo,⁶¹ K. Zeug,¹⁸⁵ C. Zhang,¹⁷ M. Zhao,¹⁷
E. Zhivun,¹⁷ G. Zhu,¹³⁸ E. D. Zimmerman,⁴⁰ M. Zito,²⁰ S. Zucchelli,¹⁹⁵ J. Zuklin,⁴³ V. Zutshi,¹³⁵ and R. Zwaska⁶¹

(The DUNE Collaboration)

¹ University of Amsterdam, NL-1098 XG Amsterdam, The Netherlands

² University of Antananarivo, Antananarivo 101, Madagascar

³ Universidad Antonio Nariño, Bogotá, Colombia

⁴ Argonne National Laboratory, Argonne, IL 60439, USA

⁵ University of Arizona, Tucson, AZ 85721, USA

⁶ Universidad Nacional de Asunción, San Lorenzo, Paraguay

⁷ University of Athens, Zografou GR 157 84, Greece

⁸ Universidad del Atlántico, Atlántico, Colombia

⁹ Banaras Hindu University, Varanasi - 221 005, India

¹⁰ University of Basel, CH-4056 Basel, Switzerland

¹¹ University of Bern, CH-3012 Bern, Switzerland

¹² Beykent University, Istanbul, Turkey

¹³ University of Birmingham, Birmingham B15 2TT, United Kingdom

¹⁴ Università del Bologna, 40127 Bologna, Italy

¹⁵ Boston University, Boston, MA 02215, USA

¹⁶ University of Bristol, Bristol BS8 1TL, United Kingdom

¹⁷ Brookhaven National Laboratory, Upton, NY 11973, USA

¹⁸ University of Bucharest, Bucharest, Romania

¹⁹ Centro Brasileiro de Pesquisas Físicas, Rio de Janeiro, RJ 22290-180, Brazil

²⁰ CEA/Saclay, IRFU Institut de Recherche sur les Lois Fondamentales de l'Univers, F-91191 Gif-sur-Yvette CEDEX, France

²¹ CERN, The European Organization for Nuclear Research, 1211 Meyrin, Switzerland

²² CIEMAT, Centro de Investigaciones Energéticas, Medioambientales y Tecnológicas, E-28040 Madrid, Spain

²³ Central University of South Bihar, Gaya – 824236, India

²⁴ University of California Berkeley, Berkeley, CA 94720, USA

²⁵ University of California Davis, Davis, CA 95616, USA

²⁶ University of California Irvine, Irvine, CA 92697, USA

²⁷ University of California Los Angeles, Los Angeles, CA 90095, USA

²⁸ University of California Riverside, Riverside CA 92521, USA

²⁹ University of California Santa Barbara, Santa Barbara, California 93106 USA

³⁰ California Institute of Technology, Pasadena, CA 91125, USA

- ³¹University of Cambridge, Cambridge CB3 0HE, United Kingdom
³²Universidade Estadual de Campinas, Campinas - SP, 13083-970, Brazil
³³Università di Catania, 2 - 95131 Catania, Italy
³⁴Institute f Particle and Nuclear Physics of the Faculty of Mathematics and Physics of the Charles University, 180 00 Prague 8, Czech Republic
³⁵University of Chicago, Chicago, IL 60637, USA
³⁶Chung-Ang University, Seoul 06974, South Korea
³⁷University of Cincinnati, Cincinnati, OH 45221, USA
³⁸Centro de Investigación y de Estudios Avanzados del Instituto Politécnico Nacional (Cinvestav), Mexico City, Mexico
³⁹Universidad de Colima, Colima, Mexico
⁴⁰University of Colorado Boulder, Boulder, CO 80309, USA
⁴¹Colorado State University, Fort Collins, CO 80523, USA
⁴²Columbia University, New York, NY 10027, USA
⁴³Institute of Physics, Czech Academy of Sciences, 182 00 Prague 8, Czech Republic
⁴⁴Czech Technical University, 115 19 Prague 1, Czech Republic
⁴⁵Dakota State University, Madison, SD 57042, USA
⁴⁶University of Dallas, Irving, TX 75062-4736, USA
⁴⁷Labratoire d'Annecy-le-Vieux de Physique des Particules, CNRS/IN2P3 and Université Savoie Mont Blanc, 74941 Annecy-le-Vieux, France
⁴⁸Daresbury Laboratory, Cheshire WA4 4AD, United Kingdom
⁴⁹Drexel University, Philadelphia, PA 19104, USA
⁵⁰Duke University, Durham, NC 27708, USA
⁵¹Durham University, Durham DH1 3LE, United Kingdom
⁵²Universidad EIA, Antioquia, Colombia
⁵³ETH Zurich, Zurich, Switzerland
⁵⁴University of Edinburgh, Edinburgh EH8 9YL, United Kingdom
⁵⁵Faculdade de Ciências da Universidade de Lisboa - FCUL, 1749-016 Lisboa, Portugal
⁵⁶Universidade Federal de Alfenas, Poços de Caldas - MG, 37715-400, Brazil
⁵⁷Universidade Federal de Goias, Goiania, GO 74690-900, Brazil
⁵⁸Universidade Federal de São Carlos, Araras - SP, 13604-900, Brazil
⁵⁹Universidade Federal do ABC, Santo André - SP, 09210-580 Brazil
⁶⁰Universidade Federal do Rio de Janeiro, Rio de Janeiro - RJ, 21941-901, Brazil
⁶¹Fermi National Accelerator Laboratory, Batavia, IL 60510, USA
⁶²University of Florida, Gainesville, FL 32611-8440, USA
⁶³Fluminense Federal University, 9 Icaraí Niterói - RJ, 24220-900, Brazil
⁶⁴Università degli Studi di Genova, Genova, Italy
⁶⁵Georgian Technical University, Tbilisi, Georgia
⁶⁶Gran Sasso Science Institute, L'Aquila, Italy
⁶⁷Laboratori Nazionali del Gran Sasso, L'Aquila AQ, Italy
⁶⁸University of Granada & CAFPE, 18002 Granada, Spain
⁶⁹University Grenoble Alpes, CNRS, Grenoble INP, LPSC-IN2P3, 38000 Grenoble, France
⁷⁰Universidad de Guanajuato, Guanajuato, C.P. 37000, Mexico
⁷¹Harish-Chandra Research Institute, Jhunsi, Allahabad 211 019, India
⁷²Harvard University, Cambridge, MA 02138, USA
⁷³University of Hawaii, Honolulu, HI 96822, USA
⁷⁴University of Houston, Houston, TX 77204, USA
⁷⁵University of Hyderabad, Gachibowli, Hyderabad - 500 046, India
⁷⁶Institut de Física d'Altes Energies, Barcelona, Spain
⁷⁷Instituto de Fisica Corpuscular, 46980 Paterna, Valencia, Spain
⁷⁸Istituto Nazionale di Fisica Nucleare Sezione di Bologna, 40127 Bologna BO, Italy
⁷⁹Istituto Nazionale di Fisica Nucleare Sezione di Catania, I-95123 Catania, Italy
⁸⁰Istituto Nazionale di Fisica Nucleare Sezione di Genova, 16146 Genova GE, Italy
⁸¹Istituto Nazionale di Fisica Nucleare Sezione di Lecce, 73100 - Lecce, Italy
⁸²Istituto Nazionale di Fisica Nucleare Sezione di Milano Bicocca, 3 - I-20126 Milano, Italy
⁸³Istituto Nazionale di Fisica Nucleare Sezione di Milano, 20133 Milano, Italy
⁸⁴Istituto Nazionale di Fisica Nucleare Sezione di Napoli, I-80126 Napoli, Italy
⁸⁵Istituto Nazionale di Fisica Nucleare Sezione di Padova, 35131 Padova, Italy
⁸⁶Istituto Nazionale di Fisica Nucleare Sezione di Pavia, I-27100 Pavia, Italy
⁸⁷Istituto Nazionale di Fisica Nucleare Laboratori Nazionali del Sud, 95123 Catania, Italy
⁸⁸Institute for Nuclear Research of the Russian Academy of Sciences, Moscow 117312, Russia
⁸⁹Institut de Physique des 2 Infinis de Lyon, 69622 Villeurbanne, France
⁹⁰Institute for Research in Fundamental Sciences, Tehran, Iran
⁹¹Instituto Superior Técnico - IST, Universidade de Lisboa, Portugal
⁹²Idaho State University, Pocatello, ID 83209, USA

- ⁹³ Illinois Institute of Technology, Chicago, IL 60616, USA
⁹⁴ Imperial College of Science Technology and Medicine, London SW7 2BZ, United Kingdom
⁹⁵ Indian Institute of Technology Guwahati, Guwahati, 781 039, India
⁹⁶ Indian Institute of Technology Hyderabad, Hyderabad, 502285, India
⁹⁷ Indiana University, Bloomington, IN 47405, USA
⁹⁸ Universidad Nacional de Ingeniería, Lima 25, Perú
⁹⁹ University of Iowa, Iowa City, IA 52242, USA
¹⁰⁰ Iowa State University, Ames, Iowa 50011, USA
¹⁰¹ Iwate University, Morioka, Iwate 020-8551, Japan
¹⁰² University of Jammu, Jammu-180006, India
¹⁰³ Jawaharlal Nehru University, New Delhi 110067, India
¹⁰⁴ Jeonbuk National University, Jeonrabuk-do 54896, South Korea
¹⁰⁵ University of Jyväskylä, FI-40014, Finland
¹⁰⁶ High Energy Accelerator Research Organization (KEK), Ibaraki, 305-0801, Japan
¹⁰⁷ Korea Institute of Science and Technology Information, Daejeon, 34141, South Korea
¹⁰⁸ K L University, Vaddeswaram, Andhra Pradesh 522502, India
¹⁰⁹ Kansas State University, Manhattan, KS 66506, USA
¹¹⁰ Kavli Institute for the Physics and Mathematics of the Universe, Kashiwa, Chiba 277-8583, Japan
¹¹¹ National Institute of Technology, Kure College, Hiroshima, 737-8506, Japan
¹¹² Kyiv National University, 01601 Kyiv, Ukraine
¹¹³ Laboratório de Instrumentação e Física Experimental de Partículas, 1649-003 Lisboa and 3004-516 Coimbra, Portugal
¹¹⁴ Laboratoire de l'Accélérateur Linéaire, 91440 Orsay, France
¹¹⁵ Lancaster University, Lancaster LA1 4YB, United Kingdom
¹¹⁶ Lawrence Berkeley National Laboratory, Berkeley, CA 94720, USA
¹¹⁷ University of Liverpool, L69 7ZE, Liverpool, United Kingdom
¹¹⁸ Los Alamos National Laboratory, Los Alamos, NM 87545, USA
¹¹⁹ Louisiana State University, Baton Rouge, LA 70803, USA
¹²⁰ University of Lucknow, Uttar Pradesh 226007, India
¹²¹ Madrid Autónoma University and IFT UAM/CSIC, 28049 Madrid, Spain
¹²² University of Manchester, Manchester M13 9PL, United Kingdom
¹²³ Massachusetts Institute of Technology, Cambridge, MA 02139, USA
¹²⁴ University of Michigan, Ann Arbor, MI 48109, USA
¹²⁵ Michigan State University, East Lansing, MI 48824, USA
¹²⁶ Università del Milano-Bicocca, 20126 Milano, Italy
¹²⁷ Università degli Studi di Milano, I-20133 Milano, Italy
¹²⁸ University of Minnesota Duluth, Duluth, MN 55812, USA
¹²⁹ University of Minnesota Twin Cities, Minneapolis, MN 55455, USA
¹³⁰ University of Mississippi, University, MS 38677 USA
¹³¹ University of New Mexico, Albuquerque, NM 87131, USA
¹³² H. Niewodniczański Institute of Nuclear Physics, Polish Academy of Sciences, Cracow, Poland
¹³³ Nikhef National Institute of Subatomic Physics, 1098 XG Amsterdam, Netherlands
¹³⁴ University of North Dakota, Grand Forks, ND 58202-8357, USA
¹³⁵ Northern Illinois University, DeKalb, Illinois 60115, USA
¹³⁶ Northwestern University, Evanston, IL 60208, USA
¹³⁷ University of Notre Dame, Notre Dame, IN 46556, USA
¹³⁸ Ohio State University, Columbus, OH 43210, USA
¹³⁹ Oregon State University, Corvallis, OR 97331, USA
¹⁴⁰ University of Oxford, Oxford, OX1 3RH, United Kingdom
¹⁴¹ Pacific Northwest National Laboratory, Richland, WA 99352, USA
¹⁴² Università degli Studi di Padova, I-35131 Padova, Italy
¹⁴³ Université de Paris, CNRS, Astroparticule et Cosmologie, F-75006, Paris, France
¹⁴⁴ Università degli Studi di Pavia, 27100 Pavia PV, Italy
¹⁴⁵ University of Pennsylvania, Philadelphia, PA 19104, USA
¹⁴⁶ Pennsylvania State University, University Park, PA 16802, USA
¹⁴⁷ Physical Research Laboratory, Ahmedabad 380 009, India
¹⁴⁸ Università di Pisa, I-56127 Pisa, Italy
¹⁴⁹ University of Pittsburgh, Pittsburgh, PA 15260, USA
¹⁵⁰ Pontificia Universidad Católica del Perú, Lima, Perú
¹⁵¹ University of Puerto Rico, Mayaguez 00681, Puerto Rico, USA
¹⁵² Punjab Agricultural University, Ludhiana 141004, India
¹⁵³ Radboud University, NL-6525 AJ Nijmegen, Netherlands
¹⁵⁴ University of Rochester, Rochester, NY 14627, USA
¹⁵⁵ Royal Holloway College London, TW20 0EX, United Kingdom
¹⁵⁶ Rutgers University, Piscataway, NJ, 08854, USA

- ¹⁵⁷ STFC Rutherford Appleton Laboratory, Didcot OX11 0QX, United Kingdom
¹⁵⁸ SLAC National Accelerator Laboratory, Menlo Park, CA 94025, USA
¹⁵⁹ Sanford Underground Research Facility, Lead, SD, 57754, USA
¹⁶⁰ Università del Salento, 73100 Lecce, Italy
¹⁶¹ Universidad Sergio Arboleda, 11022 Bogotá, Colombia
¹⁶² University of Sheffield, Sheffield S3 7RH, United Kingdom
¹⁶³ South Dakota School of Mines and Technology, Rapid City, SD 57701, USA
¹⁶⁴ South Dakota State University, Brookings, SD 57007, USA
¹⁶⁵ University of South Carolina, Columbia, SC 29208, USA
¹⁶⁶ Southern Methodist University, Dallas, TX 75275, USA
¹⁶⁷ Stony Brook University, SUNY, Stony Brook, New York 11794, USA
¹⁶⁸ University of Sussex, Brighton, BN1 9RH, United Kingdom
¹⁶⁹ Syracuse University, Syracuse, NY 13244, USA
¹⁷⁰ University of Tennessee at Knoxville, TN, 37996, USA
¹⁷¹ Texas A&M University - Corpus Christi, Corpus Christi, TX 78412, USA
¹⁷² University of Texas at Arlington, Arlington, TX 76019, USA
¹⁷³ University of Texas at Austin, Austin, TX 78712, USA
¹⁷⁴ University of Toronto, Toronto, Ontario M5S 1A1, Canada
¹⁷⁵ Tufts University, Medford, MA 02155, USA
¹⁷⁶ Universidade Federal de São Paulo, 09913-030, São Paulo, Brazil
¹⁷⁷ University College London, London, WC1E 6BT, United Kingdom
¹⁷⁸ Valley City State University, Valley City, ND 58072, USA
¹⁷⁹ Variable Energy Cyclotron Centre, 700 064 West Bengal, India
¹⁸⁰ Virginia Tech, Blacksburg, VA 24060, USA
¹⁸¹ University of Warsaw, 00-927 Warsaw, Poland
¹⁸² University of Warwick, Coventry CV4 7AL, United Kingdom
¹⁸³ Wichita State University, Wichita, KS 67260, USA
¹⁸⁴ William and Mary, Williamsburg, VA 23187, USA
¹⁸⁵ University of Wisconsin Madison, Madison, WI 53706, USA
¹⁸⁶ Yale University, New Haven, CT 06520, USA
¹⁸⁷ Yerevan Institute for Theoretical Physics and Modeling, Yerevan 0036, Armenia
¹⁸⁸ York University, Toronto M3J 1P3, Canada
¹⁸⁹ STFC Rutherford Appleton Laboratory, Didcot OX11 0QX, United Kingdom,
University of Liverpool, L69 7ZE, Liverpool, United Kingdom
¹⁹⁰ Laboratório de Instrumentação e Física Experimental de Partículas, 1649-003 Lisboa and 3004-516 Coimbra, Portugal,
Instituto Superior Técnico - IST, Universidade de Lisboa, Portugal
¹⁹¹ Laboratório de Instrumentação e Física Experimental de Partículas, 1649-003 Lisboa and 3004-516 Coimbra, Portugal,
Faculdade de Ciências da Universidade de Lisboa - FCUL, 1749-016 Lisboa, Portugal
¹⁹² University of Tennessee at Knoxville, TN, 37996, USA,
Fermi National Accelerator Laboratory, Batavia, IL 60510, USA
¹⁹³ Università di Catania, 2 - 95131 Catania, Italy,
Istituto Nazionale di Fisica Nucleare Sezione di Catania, I-95123 Catania, Italy
¹⁹⁴ Istituto Nazionale di Fisica Nucleare Sezione di Lecce, 73100 - Lecce, Italy, Università del Salento, 73100 Lecce, Italy
¹⁹⁵ Istituto Nazionale di Fisica Nucleare Sezione di Bologna, 40127
Bologna BO, Italy, Università del Bologna, 40127 Bologna, Italy
¹⁹⁶ Beykent University, Istanbul, Turkey, University of Iowa, Iowa City, IA 52242, USA
¹⁹⁷ Istituto Nazionale di Fisica Nucleare Sezione di Milano Bicocca, 3 - I-20126 Milano, Italy,
Università del Milano-Bicocca, 20126 Milano, Italy
¹⁹⁸ Fermi National Accelerator Laboratory, Batavia, IL 60510, USA, York University, Toronto M3J 1P3, Canada
¹⁹⁹ Nikhef National Institute of Subatomic Physics, 1098 XG Amsterdam, Netherlands,
University of Amsterdam, NL-1098 XG Amsterdam, The Netherlands
²⁰⁰ Istituto Nazionale di Fisica Nucleare Sezione di Genova, 16146
Genova GE, Italy, Università degli Studi di Genova, Genova, Italy
²⁰¹ Nikhef National Institute of Subatomic Physics, 1098 XG Amsterdam, Netherlands,
Radboud University, NL-6525 AJ Nijmegen, Netherlands
²⁰² Istituto Nazionale di Fisica Nucleare Sezione di Milano, 20133 Milano, Italy,
Università degli Studi di Milano, I-20133 Milano, Italy
²⁰³ University of California Berkeley, Berkeley, CA 94720, USA,
Lawrence Berkeley National Laboratory, Berkeley, CA 94720, USA
²⁰⁴ Istituto Nazionale di Fisica Nucleare Sezione di Pavia, I-27100 Pavia, Italy,
Università degli Studi di Pavia, 27100 Pavia PV, Italy
²⁰⁵ Istituto Nazionale di Fisica Nucleare Sezione di Padova, 35131 Padova, Italy,
CERN, The European Organization for Nuclear Research, 1211 Meyrin, Switzerland

²⁰⁶*University of Wisconsin Madison, Madison, WI 53706, USA,
Fermi National Accelerator Laboratory, Batavia, IL 60510, USA*

²⁰⁷*Istituto Nazionale di Fisica Nucleare Sezione di Milano, 20133 Milano, Italy,
CERN, The European Organization for Nuclear Research, 1211 Meyrin, Switzerland*

²⁰⁸*Oregon State University, Corvallis, OR 97331, USA,
Fermi National Accelerator Laboratory, Batavia, IL 60510, USA*

²⁰⁹*Central University of South Bihar, Gaya – 824236, India ,
Banaras Hindu University, Varanasi - 221 005, India*

²¹⁰*STFC Rutherford Appleton Laboratory, Didcot OX11 0QX, United Kingdom,
University of Oxford, Oxford, OX1 3RH, United Kingdom*

(Dated: December 23, 2024)

The Deep Underground Neutrino Experiment (DUNE) is a next-generation long-baseline neutrino oscillation experiment consisting of a high-power, broadband neutrino beam, a highly capable near detector located on site at Fermilab, in Batavia, Illinois, and a massive liquid argon time projection chamber (LArTPC) far detector located at the 4850L of Sanford Underground Research Facility in Lead, South Dakota. The primary scientific goals of the experiment are precise measurements of all the parameters governing long-baseline neutrino oscillation in a single experiment, sensitivity to observation of neutrinos from a core collapse supernova, and sensitivity to physics beyond the Standard Model, including baryon number violating processes. DUNE has evaluated expected sensitivity to these physics objectives; these results and the details of the simulation studies that have been performed to evaluate these sensitivities are presented in the DUNE Physics TDR [1]. The long-baseline physics sensitivity calculations presented in the DUNE TDR, and in a related physics paper [2], rely upon simulation of the neutrino beam line, simulation of neutrino interactions in the near and far detectors, fully automated event reconstruction and neutrino classification, and detailed implementation of systematic uncertainties. The purpose of this posting is to provide a simplified summary of the simulations that went into this analysis to the community, in order to facilitate phenomenological studies of long-baseline oscillation at DUNE. Simulated neutrino flux files and a GLoBES configuration describing the far detector reconstruction and selection performance are included as ancillary files to this posting. A simple analysis using these configurations in GLoBES produces sensitivity that is similar, but not identical, to the official DUNE sensitivity. DUNE welcomes those interested in performing phenomenological work as members of the collaboration, but also recognizes the benefit of making these configurations readily available to the wider community.

I. INTRODUCTION

The physics volume of the Technical Design Report (TDR)[1] for the Deep Underground Neutrino Experiment (DUNE) describes the proposed physics program for DUNE and the results of simulation studies that have been performed to quantify DUNE’s sensitivity to its physics objectives. The primary scientific objectives of DUNE are to study long-baseline neutrino oscillation to determine the neutrino mass ordering, to determine whether CP symmetry is violated in the lepton sector, and to precisely measure the parameters governing neutrino oscillation to test the three-neutrino paradigm. The DUNE physics program also includes precise measurements of neutrino interactions, sensitivity to supernova burst neutrinos, and searches for a range of physics beyond the Standard Model, including sensitivity to baryon number violating processes.

The long-baseline physics sensitivity calculations presented in the DUNE TDR and the related physics paper [2] are based upon detailed simulations of the neutrino beamline and neutrino interactions in the near and far detectors. To determine the expected physics sensitivities, a full analysis of simulation data is performed, including automated signal processing, low-level reconstruction, energy reconstruction, and event classification. This posting provides the results of some of these simulations for use by anyone in the community interested in studying long-baseline neutrino oscillation in DUNE. Simulated neutrino flux files and a GLoBES configuration describing the far detector reconstruction and selection performance are included as ancillary files to this posting. On arXiv, the ancillary files may be downloaded individually or as a gzipped tar file. The DUNE collaboration requests that any results making use of these files reference this arXiv posting and the paper describing the TDR long-baseline oscillation analysis[2].

A detailed treatment of systematics, based on the expected variations of individual systematic parameters describing uncertainties in flux, neutrino interactions, and detector effects, is included in full analysis. However, for the GLoBES files included in this posting, only simple normalization uncertainties are implemented. It is important to note that the configurations provided here are not sufficient to fully reproduce the sophisticated analysis presented in the DUNE TDR. Rather these configurations provide a simplified summary of the simulation, reconstruction, and event selection aspects of that analysis as a common starting point for phenomenological studies. The text in this document is not intended to provide thorough documentation of the details of how the TDR results were produced; that is provided in the TDR text. Rather we attempt to briefly summarize the analyses that produce these configurations and provide documentation of how the configurations may be used.

In Section II, we describe the simulated fluxes for the LBNF beamline design considered by the TDR, at both the near and far detectors, in both forward horn current (FHC) and reverse horn current (RHC) modes. These flux files are provided in the ancillary files in a directory called `dune_flux/`. In Section III, we describe the neutrino-nucleus interaction model implemented in the TDR analysis. In Section IV, we briefly describe simulation, reconstruction, and selection of the expected event samples in the far detector. The results of the far detector analysis and a greatly simplified treatment of systematic uncertainties after constraint by the near detector are provided in the ancillary files in a directory called `dune_globes/`, containing a GLoBES[3, 4] configuration, which is described in Section V.

II. FLUX SIMULATION

The neutrino fluxes used in the TDR were produced using G4LBNF, a Geant4[5, 6]-based simulation of the LBNF beamline from primary proton beam to hadron absorber. Specifically, G4LBNF version v3r5p4 was used, which was built against Geant4 version 4.10.3.p03. All simulations used the QGSP_BERT physics list.

G4LBNF is highly configurable to facilitate studies of a variety of beam options. The simulation was configured to use a detailed description of the LBNF optimized beam design [7]. That design starts with a 1.2-MW, 120-GeV primary proton beam that impinges on a 2.2m long, 16mm diameter cylindrical graphite target. Hadrons produced in the target are focused by three magnetic horns operated with 300kA currents. The target chase is followed by a 194m helium-filled decay pipe and a hadron absorber. The focusing horns can be operated in forward or reverse current configurations, creating neutrino and antineutrino beams, respectively. As described in [1], this design was motivated by a genetic algorithm used to optimize for CP-violation sensitivity. The output of the genetic algorithm was a simple design including horn conductor and target shapes, which was transformed into the detailed conceptual design simulated here by LBNF engineers. A visualization of the focusing system, as simulated in G4LBNF, is shown in Fig. 1.

The basic output of G4LBNF is a list of all particle decays to neutrinos that occur anywhere along the beamline. Weights (historically referred to as “importance weights”) are used to reduce the size of the output files by throwing out a fraction of the relatively common low-energy neutrinos while preserving less numerous high-energy neutrinos. To produce neutrino flux distributions at a particular location, all of the neutrinos in the G4LBNF output file are forced to point toward the specified location and weighted according to the relative probability that the decay in question would produce a neutrino in that direction[8].

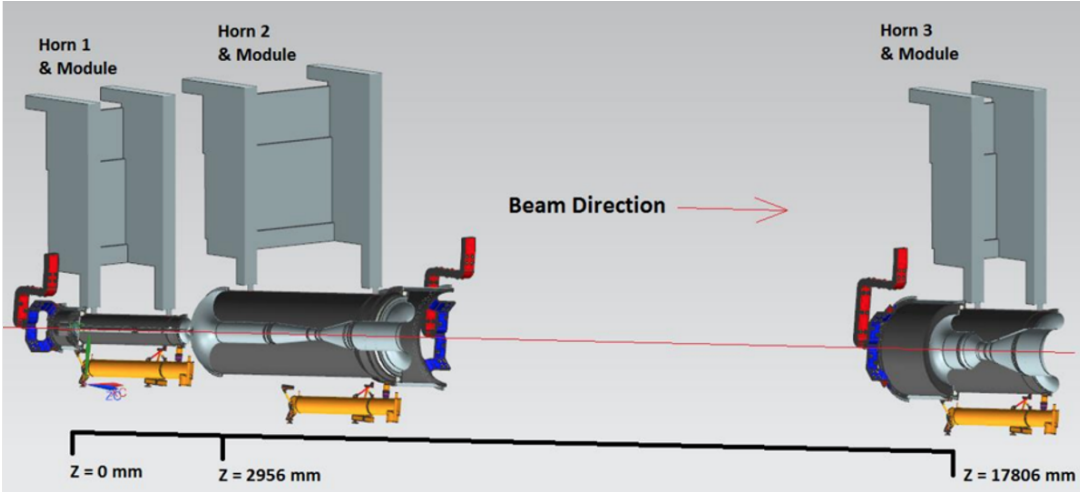


FIG. 1. Visualization (C. Crowley, FNAL) of the three-horn focusing system simulated to produce the neutrino fluxes used in the DUNE TDR and included as an ancillary file with this article.

Fluxes are provided at the center of the near detector (ND), located 474 m downstream of the start of Horn 1, and at the far detector (FD), located 1297 km downstream of the start of Horn 1. Fluxes are available for both neutrino or “forward horn current” mode (FHC) and antineutrino or “reverse horn current” mode (RHC). The simulated flux distributions at the far detector are shown in Fig. 2. Each flux is available in two formats: a root file containing flux histograms and a GLoBES flux input file. The root files also contain neutral-current and charged-current spectra, which are obtained by multiplying the flux by GENIE 2.8.4 inclusive cross sections. The flux histograms in the root files have units of neutrinos/m²/POT. Note that these histograms have variable bin widths, so discontinuities in the number of events per bin are expected. The GLoBES flux files have units of neutrinos/GeV/m²/POT. These text files are in the standard GLoBES format, in which the seven columns correspond to: E_ν , Φ_{ν_e} , Φ_{ν_μ} , Φ_{ν_τ} , $\Phi_{\bar{\nu}_e}$, $\Phi_{\bar{\nu}_\mu}$, and $\Phi_{\bar{\nu}_\tau}$. The GLoBES far detector flux files are also included as part of the provided GLoBES configuration.

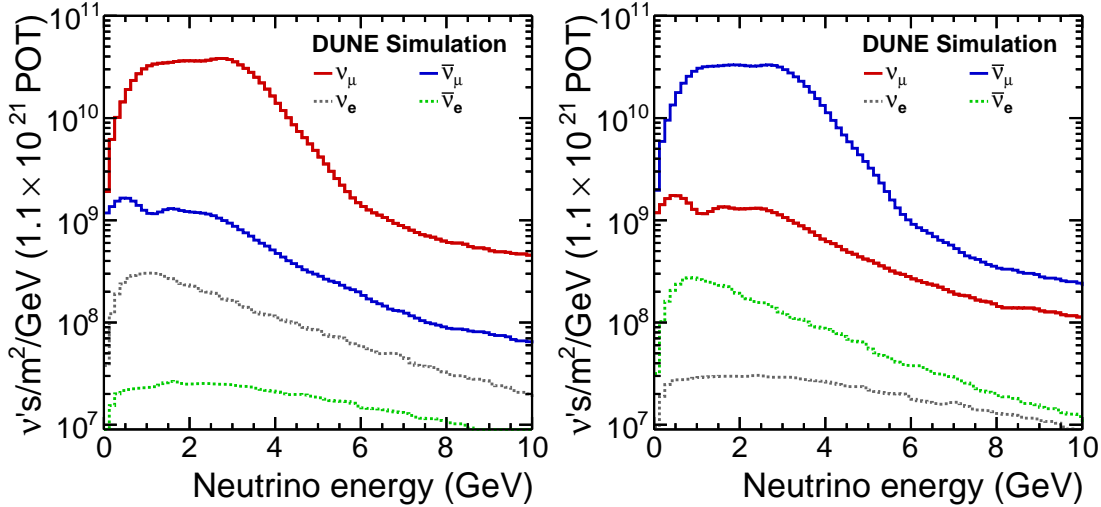


FIG. 2. Unoscillated neutrino fluxes at the far detector for neutrino-enhanced, FHC, beam running (left) and antineutrino, RHC, beam running (right). Figure reproduced from [2].

DUNE plans to measure the flux at various off-axis angles in order to access different neutrino energy spectra and use this information to reduce the model dependence of the mapping between true and reconstructed neutrino energy; this concept is referred to as DUNE PRISM. Flux histograms at off-axis angles have been generated, but are not included in the ancillary files for this posting. These additional flux files may be found at [9].

III. CROSS-SECTION SIMULATION

A model describing neutrino interactions has been implemented in v2.12.10 of the GENIE generator [10, 11]. Event weights are applied to parameterize cross-section corrections not implemented in this version of GENIE. For true charged current quasi-elastic (CCQE) interactions, the shape of the four momentum transfer is altered according to a model of the nuclear weak charge screening (RPA) calculated by the Valencia group [12], which results in a strong suppression at low four momentum transfer. In addition, the rate of resonant and non-resonant single pion production is modified according to deuterium bubble chamber tunes [13]. The resulting charged-current cross section as a function of energy is shown in Fig. 3. For more discussion on the interaction model, the reader is directed to [2]. NUISANCE [14] is used to apply weights from the DUNE reweighting framework to GENIE events and calculate the total cross sections; this output is used to produce the cross-section text files included in the GLoBES configuration supplied with this article. These cross-section text files are in the standard GLoBES format, in which the seven columns correspond to: $\log_{10}E_\nu$, $\hat{\sigma}_{\nu_e}$, $\hat{\sigma}_{\nu_\mu}$, $\hat{\sigma}_{\nu_\tau}$, $\hat{\sigma}_{\bar{\nu}_e}$, $\hat{\sigma}_{\bar{\nu}_\mu}$, and $\hat{\sigma}_{\bar{\nu}_\tau}$, where $\hat{\sigma}(E) = \sigma(E)/E[10^{-38} \frac{\text{cm}^2}{\text{GeV}}]$. Note that the ν_τ cross sections are set to zero in these files.

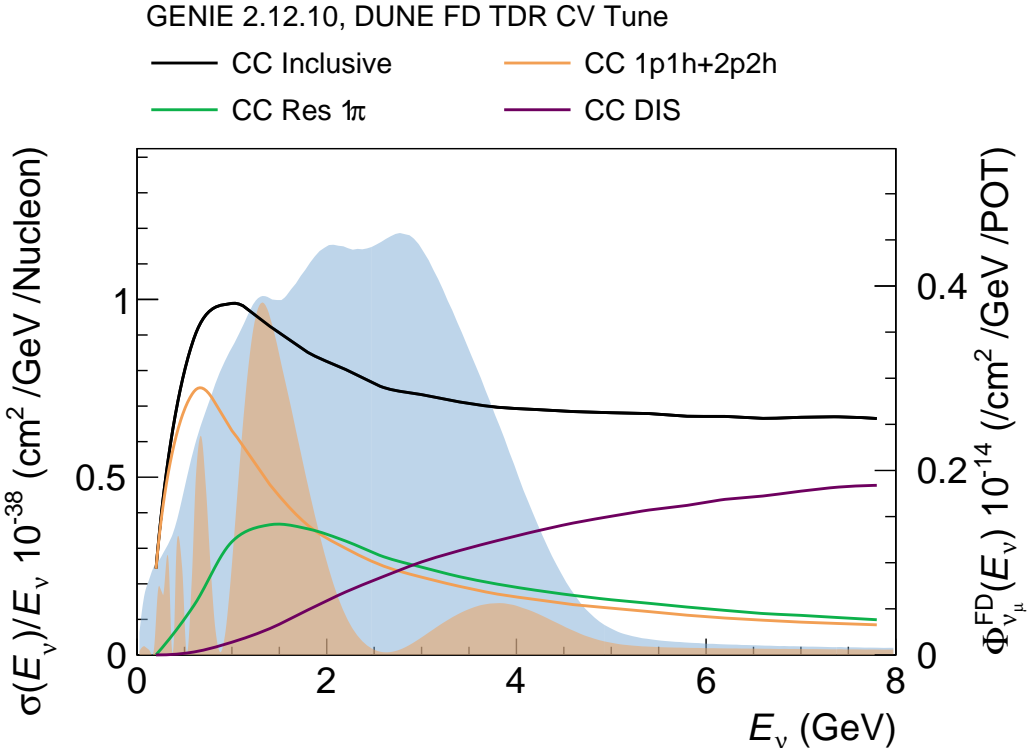


FIG. 3. Charged current neutrino interaction cross sections in the DUNE interaction model as a function of true neutrino energy. The CC inclusive (black) curve shows the cross-section values included in the GLoBES configuration. The blue and orange filled regions show the unoscillated and oscillated, respectively, ν_μ flux at the far detector for reference.

IV. MONTE CARLO ANALYSIS

As described in [2], a full analysis and event selection has been performed on simulated far detector data. Simulated data is generated using the flux and cross-section simulation tools described in the previous section and a Geant4[15] simulation of the DUNE far detector.

The electronics response to the ionization electrons and scintillation light is simulated to produce digitized signals in the wire planes and photon detectors (PDs) respectively. Raw detector signals are processed using algorithms to remove the impact of the LArTPC electric field and electronics response from the measured signal, to identify hits, and to form clusters of hits that are matched to form high-level objects such as tracks and showers.

The energy of the incoming neutrino in charged-current (CC) events is estimated by adding the lepton and hadronic energies reconstructed using the Pandora toolkit [16, 17]. If the event is selected as ν_μ CC, the muon energy is estimated from range of the longest track if it is contained in the detector and from multiple Coulomb scattering if it exits the detector. Electron and hadron energies are measured calorimetrically, with corrections applied to each hit charge for recombination and the electron lifetime. An additional correction is made to the hadronic energy to account for missing energy due to neutral particles and final-state interactions. In the energy range of 0.5 to 4 GeV that is relevant for oscillation measurements, the observed neutrino energy resolution at the far detector is \sim 15 to 20%, depending on lepton flavor and reconstruction method. It is expected that this resolution could be improved using more sophisticated reconstruction techniques, but those improvements are not considered in the analysis presented in [2] or in the GLoBES configurations provided here.

Event classification is carried out through image recognition techniques using a convolutional neural network, named convolutional visual network (CVN). A detailed description of the CVN architecture is available in [18] and the performance is discussed in [2]. CVN scores for each interaction to be a ν_μ CC or a ν_e CC interaction are obtained from a network trained on three million simulated events. The event selection requirement for an interaction to be included in the ν_e CC (ν_μ CC) sample is $P(\nu_e \text{CC}) > 0.85$ ($P(\nu_\mu \text{CC}) > 0.5$), optimized to produce the best sensitivity to CP violation. Since all of the flavor classification scores must sum to unity, the interactions selected in the two event selections are completely independent. The same selection criteria are used for both FHC and RHC beam running. The ν_e and ν_μ selection efficiencies in both FHC and RHC beam modes all exceed 90% in the neutrino flux peak.

V. GLOBES CONFIGURATION

The GLoBES configuration summarizing the result of the MC-based analysis and facilitating user-generated sensitivities is provided in the ancillary files in a directory called `dune_globes/`. Cross-section files describing charged-current and neutral-current interactions with argon, generated using GENIE v2.12.10, with weights applied to match the model choices made in the DUNE simulation, are included in the configuration. The true-to-reconstructed smearing matrices and selection efficiency as a function of reconstructed neutrino energy produced by the DUNE analysis for various signal and background modes used by GLoBES are included. The selection efficiencies are applied as a “post-smearing” efficiency in GLoBES; i.e., they are applied as a function of reconstructed neutrino energy, such that the configurations provided reproduce the event rates in Monte Carlo samples generated for the TDR analysis, including statistical fluctuations. The naming convention for the channels defined in these files is summarized in Table I. Note that while smearing and efficiency files are provided in the configurations for ν_τ interactions, the cross-sections for these events are set to zero in the provided cross-section files, so no ν_τ interactions will appear in the event rates when using the configurations as provided.

The GLoBES configuration provided in the ancillary files corresponds to 624 kt-MW-years of exposure: 6.5 years each of running in neutrino (FHC) and antineutrino (RHC) mode with a 40-kt fiducial mass far detector, in an 120-GeV, 1.2 MW beam. This is equivalent to ten years of data collection using the nominal staging assumptions described in [2]. Conversion between exposure in kt-MW-years and true years for several nominal exposures is also provided in [2]. The sensitivity calculations presented here and in the DUNE nominal analysis [2] use oscillation parameters and uncertainties based on the NuFit 4.0[19, 20] fit to global neutrino data. These central values are provided in Table II. The matter density is constant and equal to 2.848 g/cm^3 , the average matter density for this baseline [21, 22]. Figure 4 shows the expected DUNE far detector spectra produced by the GLoBES configuration provided here. These spectra are nearly identical to those produced by the full analysis, as demonstrated in Fig. 5.

In all cases, oscillation parameters are allowed to vary in the sensitivity calculations. The mixing angle θ_{13} and the solar oscillation parameters, θ_{12} and Δm_{12}^2 , are constrained by Gaussian prior functions with widths defined by the uncertainties in Table II. The uncertainty on the matter density is taken to be 2%. The GLoBES minimization is performed over both possible values for the θ_{23} octant and, in the case of CP violation sensitivity, both possible values for the neutrino mass ordering.

The ν_e and $\bar{\nu}_e$ signal modes have independent normalization uncertainties of 2% each, while the ν_μ and $\bar{\nu}_\mu$ signal modes have independent normalization uncertainties of 5%. The background normalization uncertainties range from 5% to 20% and include correlations among various sources of background; the correlations among the background normalization parameters can be seen by looking at the `@sys_on_multie_x_errors_bg` parameters in the GLoBES configurations provided with this posting. The choices for signal and background normalization uncertainties may be customized by changing the parameter values in the file `definitions.inc`. The treatment of correlation among uncertainties in this configuration requires use of GLoBES version 3.2.16, available from the GLoBES website[23]. Note that while the analysis described in the TDR *explicitly* includes selected near detector samples, the normalization

TABLE I. Description of naming convention for channels included in the GLoBES configuration provided in ancillary files. “FHC” and “RHC” appear at the beginning of each channel name and refer to “Forward Horn Current” and “Reverse Horn Current” as described in Section II. Efficiencies are provided for both the appearance mode and disappearance mode analyses.

Name Includes	Process	Description
Appearance Mode:		
app_osc_nue	$\nu_\mu \rightarrow \nu_e$ (CC)	Electron Neutrino Appearance Signal
app_osc_nuebar	$\bar{\nu}_\mu \rightarrow \bar{\nu}_e$ (CC)	Electron Antineutrino Appearance Signal
app_bkg_nue	$\nu_e \rightarrow \nu_e$ (CC)	Intrinsic Beam Electron Neutrino Background
app_bkg_nuebar	$\bar{\nu}_e \rightarrow \bar{\nu}_e$ (CC)	Intrinsic Beam Electron Antineutrino Background
app_bkg_numu	$\nu_\mu \rightarrow \nu_\mu$ (CC)	Muon Neutrino Charged-Current Background
app_bkg_numubar	$\bar{\nu}_\mu \rightarrow \bar{\nu}_\mu$ (CC)	Muon Antineutrino Charged-Current Background
app_bkg_nutau	$\nu_\tau \rightarrow \nu_\tau$ (CC)	Tau Neutrino Appearance Background
app_bkg_nutaubar	$\bar{\nu}_\tau \rightarrow \bar{\nu}_\tau$ (CC)	Tau Antineutrino Appearance Background
app_bkg_nuNC	$\nu_\mu/\nu_e \rightarrow X$ (NC)	Neutrino Neutral Current Background
app_bkg_nubarNC	$\bar{\nu}_\mu/\bar{\nu}_e \rightarrow X$ (NC)	Antineutrino Neutral Current Background
Disappearance Mode:		
dis_bkg_numu	$\nu_\mu \rightarrow \nu_\mu$ (CC)	Muon Neutrino Charged-Current Signal
dis_bkg_numubar	$\bar{\nu}_\mu \rightarrow \bar{\nu}_\mu$ (CC)	Muon Antineutrino Charged-Current Signal
dis_bkg_nutau	$\nu_\tau \rightarrow \nu_\tau$ (CC)	Tau Neutrino Appearance Background
dis_bkg_nutaubar	$\bar{\nu}_\tau \rightarrow \bar{\nu}_\tau$ (CC)	Tau Antineutrino Appearance Background
dis_bkg_nuNC	$\nu_\mu/\nu_e \rightarrow X$ (NC)	Neutrino Neutral Current Background
dis_bkg_nubarNC	$\bar{\nu}_\mu/\bar{\nu}_e \rightarrow X$ (NC)	Antineutrino Neutral Current Background

TABLE II. Central value and relative uncertainty of neutrino oscillation parameters from the NuFit 4.0 [19, 20] global fit to neutrino oscillation data. Because the probability distributions are somewhat non-Gaussian (particularly for θ_{23}), the relative uncertainty is computed using 1/6 of the $\pm 3\sigma$ allowed range from the fit, rather than the 1σ range. For some parameters, the best-fit values and uncertainties depend on whether normal mass ordering (NO) or inverted mass ordering (IO) is assumed.

Parameter	Central Value	Relative Uncertainty
θ_{12}	0.5903	2.3%
θ_{23} (NO)	0.866	4.1%
θ_{23} (IO)	0.869	4.0%
θ_{13} (NO)	0.150	1.5%
θ_{13} (IO)	0.151	1.5%
Δm_{21}^2	7.39×10^{-5} eV ²	2.8%
Δm_{32}^2 (NO)	2.451×10^{-3} eV ²	1.3%
Δm_{31}^2 (IO)	-2.512×10^{-3} eV ²	1.3%

uncertainties here were chosen to *implicitly* include the effect of the near detector and so approximate the expected uncertainty after constraints from the near detector are included.

Figure 6 shows the sensitivity of DUNE’s Asimov data to determination of the neutrino mass ordering and discovery of CP violation, based on the configurations provided here, assuming an exposure of 624 kt-MW-years. It is important to note that, due to differences in the analysis, particularly the treatment of systematic uncertainty, the sensitivity is similar, but not identical, to the official DUNE sensitivity described in [1, 2]. The sensitivity curves in Fig. 6 are provided only to assist in validation of user implementation of these configurations.

VI. SUMMARY

The results of simulations of the LBNF neutrino beamline and a full Monte Carlo simulation and analysis of expected DUNE far detector neutrino interactions are provided to facilitate phenomenological studies of DUNE physics sensitivity. The GLoBES configurations provided here produce spectra that are nearly identical to those used in the nominal DUNE TDR analysis. These configurations produce sensitivity that is similar, but not identical, to

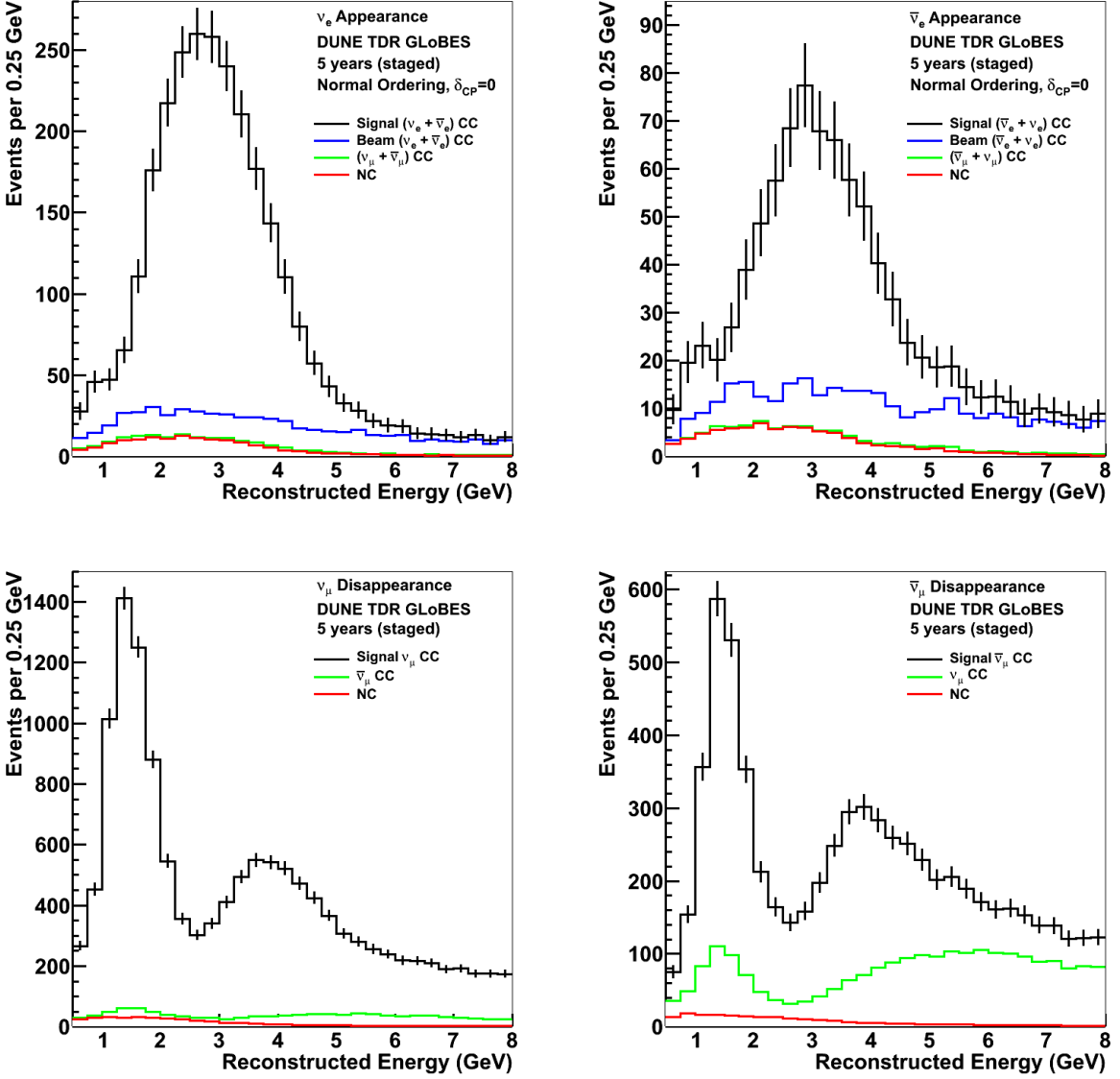


FIG. 4. Reconstructed energy distribution of selected ν_e CC-like (top) and ν_μ CC-like (bottom) events, assuming 5 years (staged) running in the neutrino-beam mode (left) and antineutrino-beam mode (right), for a total of ten years (staged) exposure. True normal ordering is assumed, $\delta_{CP}=0$, and all other oscillation parameters have the central values given in Table II. Statistical uncertainties are shown on the black histogram. Background and signal distributions are displayed as stacked histograms such that the black histogram represents the full selected sample. Spectra are generated using the GLoBES configuration provided as an ancillary file in this article.

the nominal DUNE TDR analysis for neutrino mass ordering and CP violation; the differences are primarily due to a simplified treatment of systematic uncertainty relative to that in the nominal analysis. The DUNE collaboration welcomes those interested in studying DUNE to join the collaboration or to use these configurations independently. Discussion of any results with the DUNE collaboration, either as a member or a guest, is encouraged. The collaboration requests that any results making use of the ancillary files reference this arXiv posting and the paper describing the TDR long-baseline oscillation analysis[2].

[1] DUNE, B. Abi *et al.*, (2020), 2002.03005.

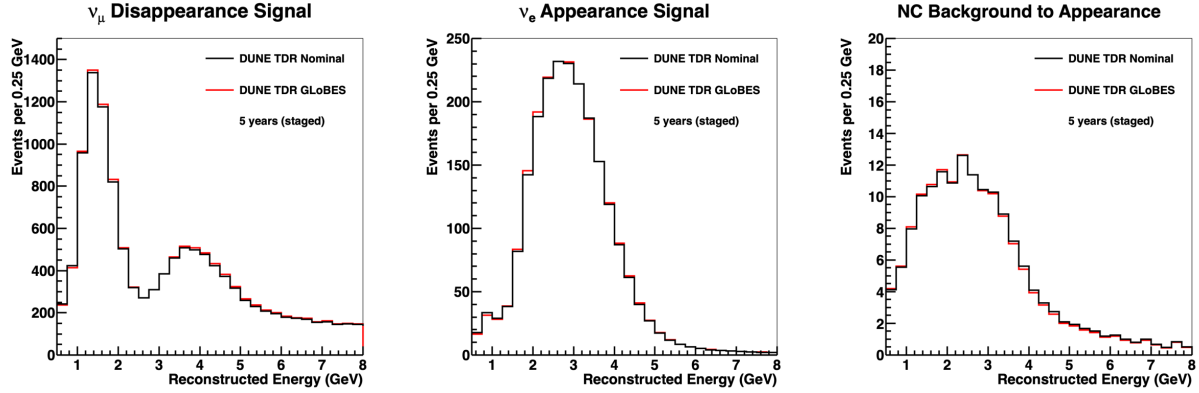


FIG. 5. Reconstructed energy distribution of selected true ν_μ CC (left), ν_e CC (middle), and neutral current (NC) background to the appearance mode (right) events, assuming 5 years (staged) running in the neutrino-beam mode. Event rates from the nominal TDR analysis (black histogram) are compared to event rates produced by the GLoBES configuration provided with this article (red histogram). True normal ordering is assumed, $\delta_{CP}=0$, and all other oscillation parameters have the central values given in Table II.

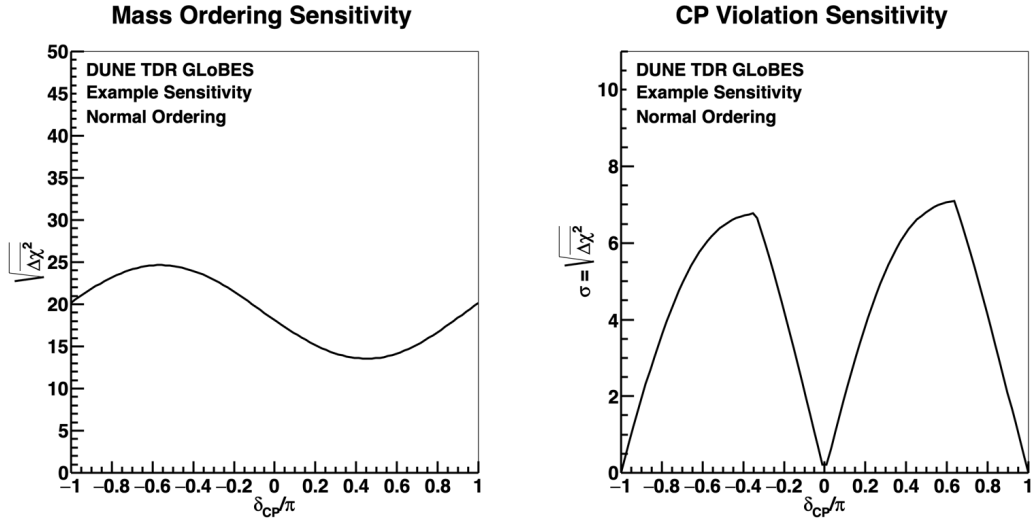


FIG. 6. The significance with which the neutrino mass ordering can be determined (left) or CP violation can be discovered (*i.e.* : $\delta_{CP} \neq 0$ or π , right) as a function of the value of δ_{CP} for an exposure of 624 kt-MW-years (10 staged years), assuming equal exposure in neutrino and antineutrino mode and true normal hierarchy, using the provided configuration and parameters given in this document.

- [2] DUNE, B. Abi *et al.*, Eur. Phys. J. C **80**, 978 (2020), 2006.16043.
- [3] P. Huber, M. Lindner, and W. Winter, Comput.Phys.Commun. **167**, 195 (2005), hep-ph/0407333.
- [4] P. Huber, J. Kopp, M. Lindner, M. Rolinec, and W. Winter, Comput.Phys.Commun. **177**, 432 (2007), hep-ph/0701187.
- [5] GEANT4, S. Agostinelli *et al.*, Nucl. Instrum. Methods A, 250 (2003).
- [6] GEANT4, J. Allison *et al.*, IEEE Trans. Nucl. Sci. **53**, 270 (2006).
- [7] P. Adamson *et al.*, The conceptual design report for the optimized neutrino beamline, 2017, <https://docs.dunescience.org/cgi-bin>ShowDocument?docid=4559>.
- [8] Z. Pavlovic, Dissertation: Measurement of neutrino oscillations with the MINOS detectors in the NuMI beam, 2009, <http://minos-docdb.fnal.gov/cgi-bin>ShowDocument?docid=5694>.
- [9] https://home.fnal.gov/~ljf26/DUNEFluxes/OptimizedEngineeredNov2017_offaxis/.
- [10] C. Andreopoulos *et al.*, Nucl. Instrum. Meth. A**614**, 87 (2010), 0905.2517.
- [11] C. Andreopoulos *et al.*, (2015), 1510.05494.
- [12] J. Nieves, J. E. Amaro, and M. Valverde, Phys. Rev. C **72**, 019902 (2005).
- [13] P. Rodrigues, C. Wilkinson, and K. McFarland, Eur. Phys. J. C **76**, 474 (2016), 1601.01888.
- [14] P. Stowell *et al.*, JINST **12**, P01016 (2017), 1612.07393.
- [15] GEANT4, S. Agostinelli *et al.*, Nucl. Instrum. Meth. A **506**, 250 (2003).

- [16] J. Marshall and M. Thomson, Pandora Particle Flow Algorithm, in *Proceedings, International Conference on Calorimetry for the High Energy Frontier (CHEF 2013)*, pp. 305–315, 2013, 1308.4537.
- [17] J. Marshall and M. Thomson, J.Phys.Conf.Ser. **396**, 022034 (2012).
- [18] DUNE, B. Abi *et al.*, Phys. Rev. D **102**, 092003 (2020), 2006.15052.
- [19] I. Esteban, M. C. Gonzalez-Garcia, A. Hernandez-Cabezudo, M. Maltoni, and T. Schwetz, JHEP **01**, 106 (2019), 1811.05487.
- [20] I. Esteban, M. C. Gonzalez-Garcia, A. Hernandez-Cabezudo, M. Maltoni, and T. Schwetz, Nufit4.0, 2018.
- [21] W. Shen and M. H. Ritzwoller, Journal of Geophysical Research: Solid Earth **121**, 4306 (2016), <https://agupubs.onlinelibrary.wiley.com/doi/pdf/10.1002/2016JB012887>.
- [22] B. Roe, Phys. Rev. **D95**, 113004 (2017), 1707.02322.
- [23] GLoBES, <https://www.mpi-hd.mpg.de/personalhomes/globes/>.